

Preclinical Evaluation of a New, Stabilized Neurotensin(8–13) Pseudopeptide Radiolabeled with ^{99m}Tc

Elisa García-Garayoa, PhD¹; Peter Bläuenstein, PhD¹; Matthias Bruehlmeier, MD¹; Alain Blanc, BChE¹; Koen Iterbeke, PhD²; Peter Conrath, PhD²; Dirk Tourwé, PhD²; and P. August Schubiger, PhD¹

¹Center for Radiopharmaceutical Science, Paul Scherrer Institute, Villigen, Switzerland; and ²Department of Organic Chemistry, Vrije Universiteit Brussel, Brussels, Belgium

The rapid degradation of neurotensin (NT) limits its clinical use in cancer imaging and therapy. Thus, a new NT(8–13) pseudopeptide, NT-VIII, was synthesized. Some changes were introduced in the sequence of NT(8–13) to stabilize the molecule against enzymatic degradation: Arg⁸ was *N*-methylated, and Lys and Ile replaced Arg⁹ and Ile¹², respectively. Finally, (N α His)Ac was coupled to the *N*-terminus for $^{99m}\text{Tc}(\text{CO})_3$ labeling. This peptide was characterized both *in vitro* and *in vivo*.

Methods: The new analog was labeled with $^{99m}\text{Tc}(\text{CO})_3$. Its metabolic stability was analyzed both in human plasma and in HT-29 cells. Binding properties, receptor downregulation, and internalization were tested with HT-29 cells. Biodistribution was evaluated in nude mice with HT-29 xenografts. **Results:** $^{99m}\text{Tc}(\text{CO})_3\text{NT-VIII}$ showed a high stability in plasma, where most of the peptide remained intact after 24 h of incubation at 37°C. However, the degradation in HT-29 cells was more rapid (46% of intact $^{99m}\text{Tc}(\text{CO})_3\text{NT-VIII}$ after 24 h at 37°C). Binding to NT1 receptors (NTR1) was saturable and specific. Scatchard analysis showed a high affinity for $^{99m}\text{Tc}(\text{CO})_3\text{NT-VIII}$, with a dissociation constant similar to $^{125}\text{I-NT}$ (1.8 vs. 1.6 nmol/L). After interacting with NTR1, $^{99m}\text{Tc}(\text{CO})_3\text{NT-VIII}$ was rapidly internalized, with more than 90% internalized after 30 min. It also distributed and cleared rapidly in nude mice bearing HT-29 xenografts. The highest rates of accumulation were found in kidney and tumor at all time points tested. Tumor uptake was highly specific because it could be blocked by coinjection with a high dose of (N α His)Ac-NT(8–13). Tumors were clearly visualized in scintigraphy images. **Conclusion:** The changes that were introduced stabilized the molecule against enzymatic degradation without affecting binding properties. Moreover, the increase in stability enhanced tumor uptake, making this derivative a promising candidate for clinical use.

Key Words: neurotensin(8–13); internalization; biodistribution; scintigraphy; metabolic stability

J Nucl Med 2002; 43:374–383

High-affinity neuropeptide receptors are expressed in high concentrations in several human tumors. The overexpression of neuropeptide receptors in malignant tumors makes them an attractive target for use in imaging or therapy that applies specific radiolabeled ligands (1–3). Thus, small peptides that bind these cell-surface receptors with high affinity have been the focus of many investigations in the last few years (4–8).

NT (pGlu-Leu-Tyr-Glu-Asn-Lys-Pro-Arg-Arg-Pro-Tyr-Ile-Leu) is a tridecapeptide that was first isolated from bovine hypothalamus (9). In mammals, NT is localized in both the central nervous system and peripheral tissues (mainly in the gastrointestinal tract), acting as both a neurotransmitter and a local hormone (10–12). The biologic effect of NT results from the specific interaction of the peptide with cell-surface receptors. At present, 2 binding sites have been characterized for NT: NT receptor subtype 1 (NTR1), which shows high affinity and low capacity, and NT receptor subtype 2 (NTR2), which shows low affinity and high capacity (13,14) and can be blocked by levocabastine, a histamine-1 receptor antagonist (15). Both NTR1 and NTR2 are G protein-coupled receptors with 7 putative transmembrane domains. Recently, a new subtype was reported, but its physiologic functions remain unknown (16).

As shown by Reubi et al. (17), NT receptors are known to be overexpressed in a variety of human tumors, such as Ewing's sarcoma (65%), meningioma (52%), astrocytoma (43%), medulloblastoma (38%), medullary thyroid carcinoma (29%), and small cell lung cancer (25%).

As already described (3), the use of small peptides has advantages over monoclonal antibodies for tumor imaging, such as easier synthesis and modification, high affinity, and rapid plasma clearance, which may result in a high concentration in the target tissue and therefore better tumor-to-background ratios. However, peptides are rapidly metabolized in plasma by endogenous peptidases, terminating their biologic effect under physiologic conditions. The 2 main cleavage bonds in the metabolic deactivation of NT(8–13) are Arg⁸–Arg⁹ and Tyr¹¹–Ile¹² (18,19). These 2 bonds

Received May 23, 2001; revision accepted Nov. 19, 2001.
For correspondence or reprints contact: P. August Schubiger, PhD, Center for Radiopharmaceutical Science, Paul Scherrer Institute, CH-5232 Villigen PSI, Switzerland.
E-mail: schubiger@psi.ch

should be stabilized to prolong the half-life of the peptide and, thus, increase the chances of reaching the tumor and binding to the receptors.

Here, we present a new, promising NT pseudopeptide, NT-VIII. The basic sequence was fragment 8–13 of NT, to which some modifications were introduced to improve metabolic stability. The molecule of NT-VIII (Fig. 1) was obtained after *N*-methylation of Arg⁸ and replacement of Arg⁹ by Lys and Ile¹² by Tle. This sequence has been previously reported by Heyl et al. (20). Finally, (N α His)Ac was linked to the amine terminus (Arg⁸) as a tridentate ligand, which is optimal for labeling with ^{99m}Tc(CO)₃, as described by Schibli et al. (21). In this article, we report the binding properties, internalization, downregulation, and in vitro stability of this new pseudopeptide, as well as its in vivo biodistribution in nude mice bearing human HT-29 colon adenocarcinoma xenografts.

MATERIALS AND METHODS

Chemicals

Chemicals for the assays were obtained from various sources. McCoy's 5A and GlutaMAX-I culture media, fetal bovine serum, antibiotic/antimycotic solution, trypsin/ethylenediaminetetraacetic acid (EDTA), bovine serum albumin, and soybean trypsin inhibitor were from Gibco BRL Life Technologies AG (Basel, Switzerland). [¹²⁵I]Tyr³-NT was from Amersham (Zurich, Switzerland). *N*-2-Hydroxyethylpiperazine-*N'*-2-ethanesulfonic acid (HEPES), chymostatin, bacitracin, and neurotensin (NT) fragment 8–13 were from Sigma (Buchs, Switzerland). Ethylene glycol-bis(β -aminoethyl ether)-*N,N,N',N'*-tetraacetic acid (EGTA), morpholinoethanesulfonic acid, *N,N,N',N'*-tetramethyl-*O*-(benzotriazol-1-yl)uronium tetrafluoroborate (TBTU), *N*-methylmorpholine, and glycine were from Fluka (Buchs, Switzerland). HF, HCl, NaCl, MgCl₂, NaOH, and KCl were from Merck (Dietikon, Switzerland). The ⁹⁹Mo/^{99m}Tc generator was from Mallinckrodt (Petten, The Netherlands).

Synthesis of New NT(8–13) Derivative and Radiolabeling

Peptide solid-phase synthesis was performed on a Merrifield resin, using a semiautomatic Peptide Synthesizer SP640B (Labor-

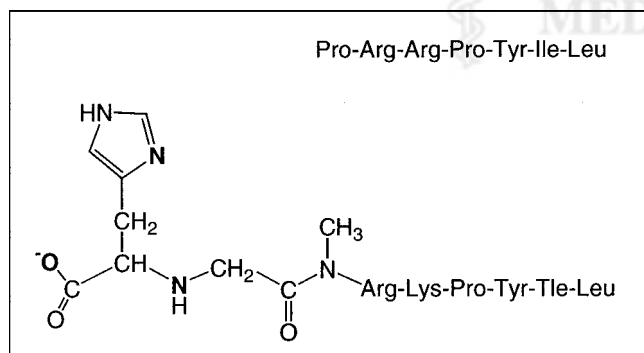


FIGURE 1. Sequence of NT-VIII (bottom), compared with NT(7–13) (top). Atoms in boldface represent ligands for metal complex formation with ^{99m}Tc(CO)₃⁺ and ^{nat}Re(CO)₃⁺. nat = natural isotopes 185/187.

tec, Bubendorf, Switzerland). Tert-butyloxycarbonyl main-chain protected amino acids were used. Couplings were performed for 2 h with 4 Eq of TBTU as the coupling reagent, 4 Eq protected amino acid, and 20 Eq *N*-methylmorpholine as the base. The (N α His)Ac was attached in a way similar to that of the former analogs. Cleavage from the resin was done using hydrogenfluoric acid in the presence of anisole. Mass spectra were recorded on a VG Quattro II spectrometer (electrospray ionization; cone voltage, 70 V; Micromass, Manchester, U.K.). Data were collected with MassLynx software (Waters, Milford, MA). ^{99m}Tc(CO)₃ was radiolabeled according to a recently described method (21), with few modifications. Briefly, 1–10 GBq pertechnetate in approximately 2 mL generator eluate were added to a mixture of 4 mg sodium carbonate, 5.5 mg sodium borohydride, and 15 mg sodium potassium tartrate in a penicillin vial under a carbon monoxide atmosphere and heated at 75°C for at least 30 min. The solution was cooled and neutralized (pH 6.5–7.5) using morpholinoethanesulfonic acid and hydrochloric acid. Immediately afterward, 0.2–0.5 mL of the neutralized technetium carbonyl solution was mixed with 10–25 μ L of a 0.001 mol/L solution of NT-VIII (minimal final concentration, 0.05 mmol/L) and again heated to 75°C for at least 1 h. The product was analyzed and purified with high performance liquid chromatography (HPLC) using an RP-18 reversed-phase column. Solvent A was 0.1% trifluoroacetic acid in water, solvent B was 70:30 ethanol:water and 0.1% trifluoroacetic acid (pH 2–2.5). A gradient with solvents A and B was run as follows: 0–3 min, 100% A; 3–15 min, 100%–50% A and 0%–50% B; after 15 min, 50% A and 50% B.

During purification, 1-mL fractions were taken. For the binding assays, the fraction with the highest activity was used because high concentrations of peptide were needed to reach saturation. This fraction was neutralized with 1 mol/L NaOH.

The cold (^{nat}Re)(CO)₃NT-VIII, where nat = natural isotopes 185/187, was synthesized and purified with HPLC under the same conditions as those used for ^{99m}Tc labeling, starting from [NEt₄]₂[ReBr₃(CO)₃] (22), but was heated overnight (\geq 8 h) instead of for 1 h. The product was characterized with a matrix-assisted laser desorption/ionization time-of-flight mass spectrometer.

Cell Culture

A human colon adenocarcinoma HT-29 cell line was obtained from European Collection of Cell Culture (Salisbury, England). Cells were maintained in McCoy's 5A and GlutaMAX-I media supplemented with 10% fetal bovine serum, 100 IU/mL penicillin, 100 μ g/mL streptomycin, and 0.25 μ g/mL amphotericin B. The cells were cultured at 37°C in a humidified incubator under an atmosphere containing 7.5% CO₂ and passaged weekly.

Metabolic Stability in Human Plasma and HT-29 Cells

Metabolic stability was analyzed in human plasma and HT-29 cells. Plasma samples from healthy donors were incubated with ^{99m}Tc(CO)₃NT-VIII at a concentration of 0.2 pmol/mL at different times (up to 24 h). After incubation, the plasma samples were centrifuged at 4°C (14,000g for 10 min), the pellet was discarded, and a sample of the supernatant was injected into a Superdex peptide column (Pharmacia, Piscataway, NJ) for fast protein liquid chromatography separation. For the experiments performed with HT-29 cells, adherent cells at confluence in 25-cm² culture flasks were incubated with 0.2 pmol/mL ^{99m}Tc(CO)₃NT-VIII. The concentration of total [⁹⁹ + ^{99m}Tc]NT-VIII was calculated as described by Bauer and Pabst (23). The cells were incubated with 3.7

MBq/mL, corresponding to a concentration of 0.2 pmol/mL. The amount of activity taken up was $10\% \pm 2\%$ of the total activity added. At different time points (up to 24 h), a sample of the culture medium was injected for fast protein liquid chromatography separation. In both cases, 0.5-mL (30 s) fractions were collected and the eluted radioactivity was determined in an NaI γ -counter (Packard Instrument Co., Inc., Downers Grove, IL).

Binding Assays

Binding assays were performed on whole HT-29 cells at confluence. A day before the assay, cells (10^6 cells/0.4 mL, equivalent to 0.3 mg protein) were placed in 48-well plates. A special binding buffer that includes protease inhibitors (50 mmol/L HEPES, 125 mmol/L NaCl, 7.5 mmol/L KCl, 5.5 mmol/L $MgCl_2$, 1 mmol/L EGTA, 5 g/L bovine serum albumin, 2 mg/L chymostatin, 100 mg/L soybean trypsin inhibitor, 50 mg/L bacitracin, pH 7.4) was used for the experiments. In inhibition studies, cells were incubated for 1 h at 37°C in triplicate with 25,000 cpm of ^{125}I -NT and variable concentrations (0.001–3,000 nmol/L) of unlabeled NT(8–13), unlabeled NT-VIII, or NT-VIII labeled with ^{nat}Re (final volume of 0.2 mL per well). The cells were then washed twice with cold binding buffer and afterward were solubilized with 1N NaOH at 37°C (0.4 mL per well). The activity was determined in a γ -counter. In saturation studies, cells were incubated in triplicate with increasing concentrations (0.1–10 nmol/L) of $^{99m}Tc(CO)_3NT$ -VIII for 1 h at 37°C (final volume, 0.2 mL per well). The concentrations of total technetium ($^{99} + ^{99m}Tc$), calculated as described by Bauer and Pabst (23), were equivalent to 0.2–20 MBq ^{99m}Tc activity per well. After 2 washings with the same binding buffer as before, the cells were then solubilized with 1N NaOH at 37°C (0.4 mL per well). The bound radioactivity was measured in the γ -counter. Nonspecific binding was determined with 1 μ mol/L unlabeled NT(8–13).

Internalization and Receptor Downregulation

Studies of internalization of receptor-bound $^{99m}Tc(CO)_3NT$ -VIII were performed as previously described (24,25), with some modifications. Briefly, HT-29 cells at confluence were placed in 6-well plates. The cells were incubated with approximately 4 kBq $^{99m}Tc(CO)_3NT$ -VIII in culture medium for 5, 15, 30, 60, and 120 min at 37°C to allow binding and internalization (total final volume, 1 mL per well). Nonspecific internalization was evaluated in the presence of 1 μ mol/L unlabeled NT(8–13). After the various incubation times, the cells were washed 3 times with ice-cold culture medium to discard unbound peptide. Surface-bound activity was removed by 2 acid washes of 5 min each (50 mmol/L glycine-HCl, 100 mmol/L NaCl, pH 2.8, 0.6 mL per well) at room temperature. Finally, the amount of internalized activity was recovered by solubilizing cells with 0.6 mL per well of 1N NaOH at 37°C. Surface-bound and internalized activities were measured in a γ -counter. Other experiments were performed with incubation at 4°C for 2 h followed by incubation at 37°C (from 5 min to 2 h). Internalization of the bound activity was then measured as described above. All experiments were performed in triplicate. The results are expressed as percentage of internalized activity related to the total activity associated with cells (surface bound plus internalized).

Downregulation tests were performed as described by Hermans et al. (26). Briefly, HT-29 cells at confluence were placed in 12-well plates and were incubated in triplicate with NT(8–13) and NT-VIII at a concentration of 3 nmol/L in the previ-

ously described binding buffer (final volume, 1 mL per well). Control wells contained only binding buffer. The first incubation was performed at 37°C for 5, 15, and 30 min. The cells were then incubated with ^{125}I -NT for 45 min. Excess of unbound ^{125}I -NT was washed with binding buffer twice. Finally, the cells were detached with 0.5 mL NaOH, 1N, and the radioactivity was measured in a γ -counter. Two additional plates were also incubated with NT(8–13) and NT-VIII for 30 min, then washed twice with binding buffer and maintained at 37°C with culture medium for 4 and 24 h to analyze the recovery of binding capacity. The results are expressed as percentage related to total binding found in control wells.

Biodistribution Studies

Female CD-1 nu/nu mice (6 to 8 wk old) bearing human HT-29 colon adenocarcinoma xenografts were used. For induction of tumor xenografts, HT-29 cells at a concentration of 8×10^6 cells per mouse were injected subcutaneously and allowed to grow for 10 d. On the day of the assay, each mouse received 3.5–4 MBq $^{99m}Tc(CO)_3NT$ -VIII through the tail vein. The mice were killed by cervical dislocation at 5 different postinjection times (1.5, 3, 5, 15, and 24 h) and then were dissected. The amount of radioactivity in tumor and other tissues (blood, heart, lung, spleen, liver, kidney, stomach, intestine, and brain) was determined by γ -counting. Three to 6 mice per time point were used. The results are expressed as percentage of injected dose per gram of tissue (%ID/g) by reference to standards prepared from dilutions of the injected preparation.

In blockade experiments, each mouse received 3.5–4 MBq $^{99m}Tc(CO)_3NT$ -VIII intravenously, coinjected with a dose of 0.3 mg cold ($N\alpha$ His)Ac-NT(8–13), which is the analog NT-II of the same series (25,27). The animals were killed at 1.5 h after injection, the organs were removed, and the radioactivity per organ was measured in the γ -counter.

Additionally, scintigraphy images were made of the mice killed at 1.5 h after injection of $^{99m}Tc(CO)_3NT$ -VIII. In these mice, 2 different tumor xenografts were induced. Each animal received a subcutaneous injection of 8×10^6 cells of both human colonic carcinoma HT-29 (in the neck area) and human prostatic carci-

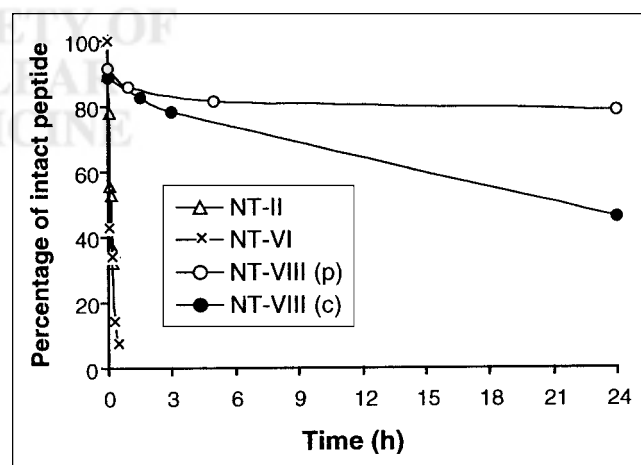


FIGURE 2. Degradation of NT-VIII in vitro after incubation at 37°C, compared with nonstabilized analog NT-II and monostabilized analog NT-VI (25). Data represent mean of 2 experiments.

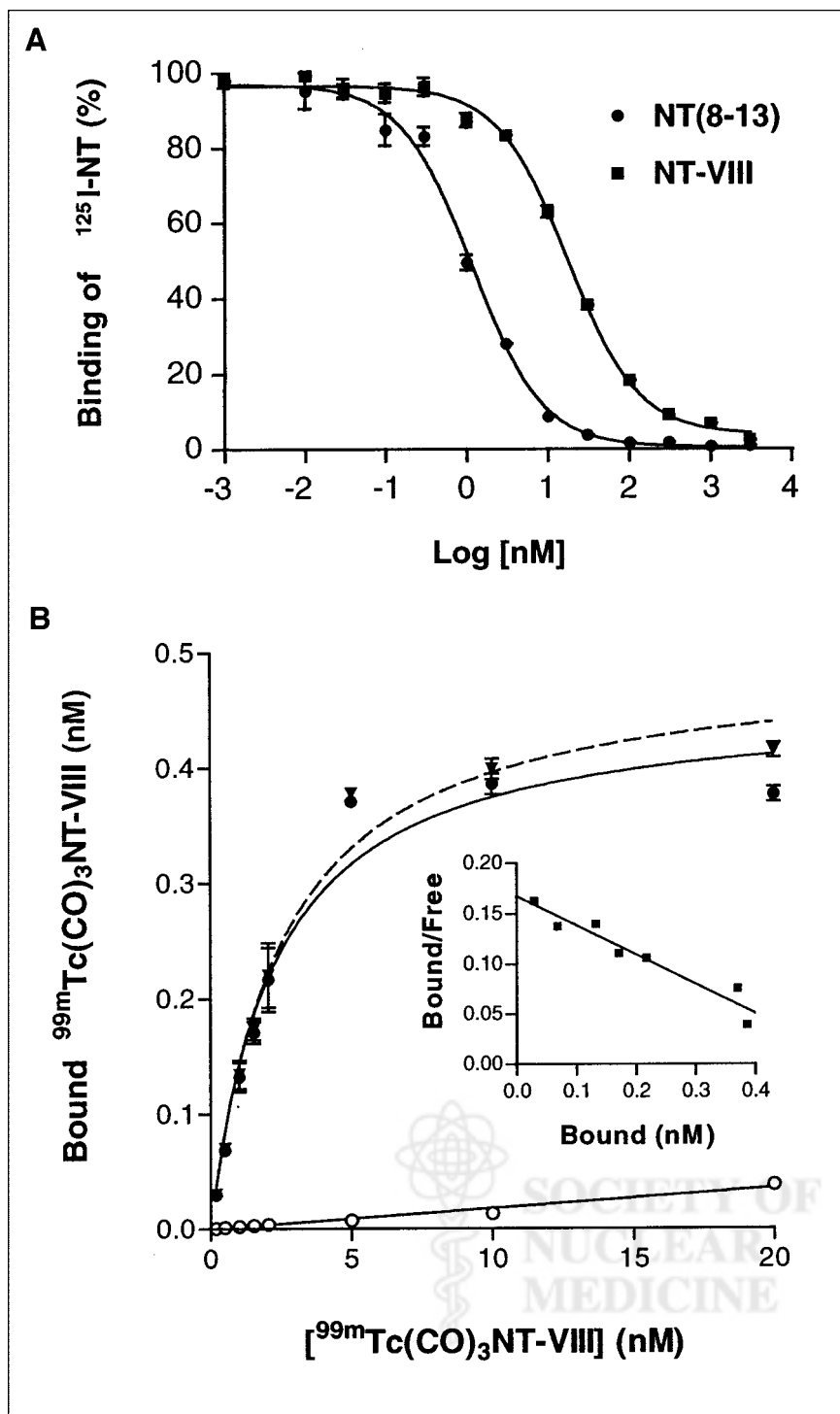


FIGURE 3. Binding of analog NT-VIII to human colon adenocarcinoma HT-29 cells. (A) Inhibition of specific binding of $^{125}\text{I-NT}$ by increasing concentrations of NT(8-13) and NT-VIII. (B) Saturation curve for $^{99\text{m}}\text{Tc}(\text{CO})_3\text{NT-VIII}$ in absence (\blacktriangle , total binding) or presence (\circ , nonspecific binding) of $1\ \mu\text{mol/L}$ unlabeled NT(8-13) for 1 h at 37°C . Specific binding (\bullet) was calculated as difference between total and nonspecific binding. Small graph shows Scatchard analysis of data. Each point is mean of triplicate determinations from representative experiment of total of 3 separate experiments.

noma PC-3 cells (in the hip area), the latter expressing both high-affinity NTR1 and low-affinity NTR2. Images were obtained on a small-field single-head Basicam gamma camera (29-cm-diameter field of view; Siemens Medical Systems, Inc., Hoffman Estates, IL). Acquisition was performed in zoomed mode, using a low-energy general-purpose parallel-hole collimator. Planar images were obtained in ventral and dorsal views. Approximately 50,000 counts were collected during the 10-min acquisition time per view.

RESULTS

Synthesis of New NT(8-13) Derivative and Radiolabeling

The structure of the new NT(8-13) derivative, NT-VIII, is shown in Figure 1. The retention time in HPLC was 17.5 min. The main peak obtained in the mass spectra corresponded to a molecular mass of 998 (molecular weight = $997 [\text{NT-VIII} + 1\ \text{H}^+]$).

After labeling, yields > 90% were reached. The yield was lower, though, when the incubation time was shorter than 1 h, but the yield did not change significantly with increase of incubation time. One main product, which corresponded to $^{99m}\text{Tc}(\text{CO})_3\text{NT-VIII}$, was obtained after labeling. This compound was analyzed by HPLC, retention time being 23 min. The concentration of unlabeled peptide was 1,000-fold higher than that of labeled peptide. Both pertechnetate and tricarbonyl represented up to 5% and 1%, respectively, of the total activity. After purification, pertechnetate and tricarbonyl were not detectable. The remaining amount of cold peptide was also not detectable by ultraviolet analysis.

^{nat}Re -labeled NT-VIII was analyzed by HPLC. Retention time on HPLC was identical for both the technetium and the rhenium products. The mass spectrometry of $^{nat}\text{Re}(\text{CO})_3\text{NT-VIII}$ confirmed the correct structure, showing 2 main peaks at 1,294 and 1,296, corresponding to the natural isotopes ^{185}Re and ^{187}Re (peak intensities according to the natural abundance of these nuclides), respectively, and 2 minor peaks at 1,295 and 1,297, corresponding to a protonated form of the product.

Metabolic Stability in Human Plasma and HT-29 Cells

The stability of the new pseudopeptide was tested both in human plasma and in HT-29 cells. $^{99m}\text{Tc}(\text{CO})_3\text{NT-VIII}$ proved to be stable in human plasma, with most of the peptide still intact after 24 h of incubation at 37°C. In HT-29 cells, however, a quicker degradation was found, and 54% of the peptide was already metabolized after 24 h of incubation. Figure 2 summarizes the results.

Binding Assays

In inhibition studies, NT-VIII inhibited the binding of ^{125}I -NT, showing a typical sigmoid curve (Fig. 3A). The inhibitory concentration of 50% (IC_{50}) obtained for NT-VIII (21.1 nmol/L) was approximately 15 times higher than that observed for fragment 8–13 of NT (1.5 nmol/L), indicating a lower affinity for NT receptors in this cell line (Fig. 3A). However, after NT-VIII was labeled with ^{nat}Re , a higher affinity was found (IC_{50} of 7.3 nmol/L). In saturation studies, specific binding of ^{125}I -NT and $^{99m}\text{Tc}(\text{CO})_3\text{NT-VIII}$ to intact cells was found to be saturable and highly specific

TABLE 1
Binding Properties of NT-VIII in HT-29 Cells

Peptide	IC_{50}^* (nmol/L)	K_d (nmol/L)
NT	0.9 [†]	1.6
NT-VIII	21.1	1.8
$^{nat}\text{Re}(\text{CO})_3\text{NT-VIII}$	7.3	—

*Displacement of ^{125}I -NT binding.

[†]Value for NT(8–13).

Data are from 2–3 experiments in triplicate. K_d was determined with ^{125}I -NT and $^{99m}\text{Tc}(\text{CO})_3\text{NT-VIII}$.

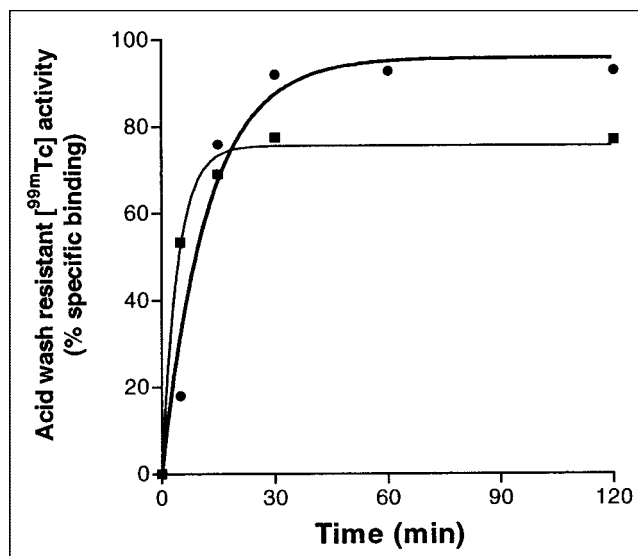


FIGURE 4. Time course internalization of $^{99m}\text{Tc}(\text{CO})_3\text{NT-VIII}$ in HT-29 cells at 37°C with (■) and without (●) preincubation at 4°C. Data are percentage of acid-resistant activity related to total activity in cells (surface-bound and internalized). Each point represents mean of 2–3 experiments in triplicate.

(Fig. 3B). The dissociation constant (K_d) obtained for $^{99m}\text{Tc}(\text{CO})_3\text{NT-VIII}$ (1.8 nmol/L) was similar to that obtained for ^{125}I -NT (1.6 nmol/L) in this cell line, showing a similar affinity for both peptides. Table 1 summarizes the results.

Internalization and Receptor Downregulation

NTR1 is rapidly internalized after stimulation with agonists, a fact that has already been reported for NT in various cells (28,29). In our experiments, we also found rapid internalization of the surface-bound $^{99m}\text{Tc}(\text{CO})_3\text{NT-VIII}$ into HT-29 cells. More than 50% of the peptide had already been internalized by incubation at 37°C for 5 min after previous incubation at 4°C. This percentage increased to 70% after 30 min at 37°C and then slowed to 80% after 60 min. The level of internalized activity remained constant for at least 2 h. In the experiments performed without the 4°C preincubation, the internalization was also found to be time dependent. It sharply increased during the first 30 min, reaching its maximal internalization levels of >90%. It also remained stable after 2 h. Figure 4 shows the results.

Incubation of HT-29 cells at 37°C with 3 nmol/L of the parent NT(8–13) as reference induced a time-dependent reduction in the amount of membrane NTR1, with a maximal decrease after 30 min of incubation. At that time, the binding capacity was reduced by $32.2\% \pm 4.6\%$. Reappearance of receptors at the cell surface after their internalization was also time dependent. After 4 h, the total binding increased to 80%, whereas at 24 h the binding capacity was approximately 92% of the control value (Fig. 5). In the case of NT-VIII also, at 3 nmol/L the reduction in binding capacity was only $13.3\% \pm 12.1\%$ after 30 min of incuba-

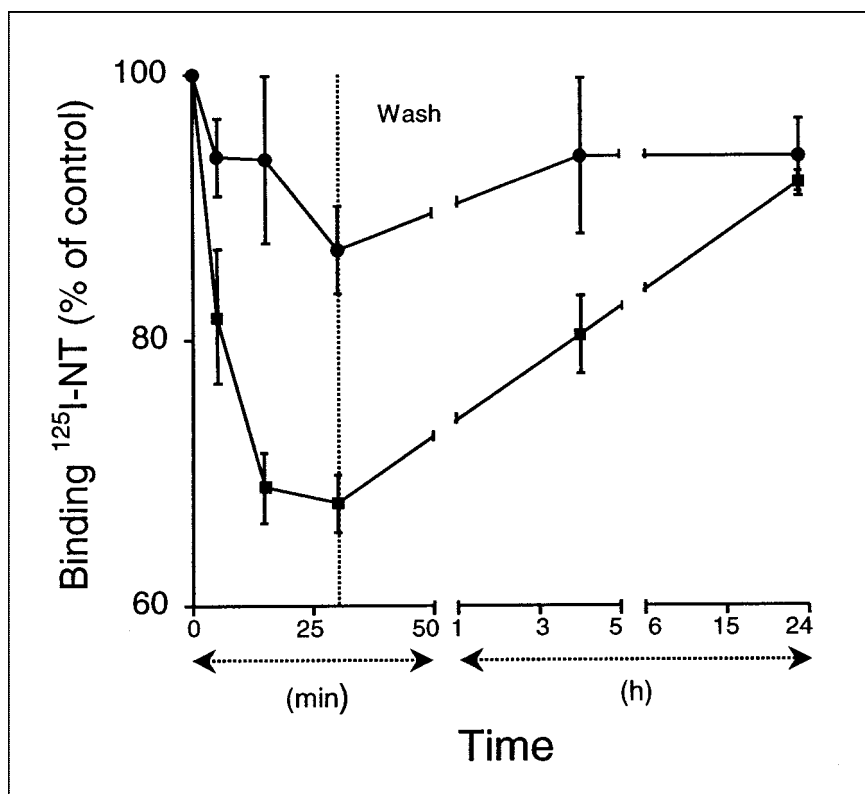


FIGURE 5. Time-dependent downregulation and subsequent reappearance of NT receptors in HT-29 cells after incubation with NT(8-13) (●) and NT-VIII (■) at concentration of 3 nmol/L. Results are percentage of maximal binding in control cells and represent mean \pm SD of 2-3 experiments in triplicate.

tion. The highest binding capacity recovery was 94% after 4 h (Fig. 5).

Biodistribution Studies

In the biodistribution studies performed with $^{99m}\text{Tc}(\text{CO})_3\text{NT-VIII}$, rapid clearance from the blood pool was observed in nude mice with tumor xenografts. At 1.5 h after injection, uptake in the tumor was 3.9 ± 1.1 %ID/g, the second highest accumulation after that in the kidneys (8.3 ± 2.9 %ID/g). Uptake in the remaining organs was $<1.5\%$, except in the liver, where an uptake of 2.8 ± 1.7 %ID/g was found at that time point (Fig. 6). In some animals, both HT-29 and PC-3 tumor xenografts were induced. Both tumors could clearly be visualized through scintigraphy at 1.5 h after injection (Fig. 7). A nonsignificant decrease in uptake at 3 h after injection and an increase at 5 h after injection were observed. After 15 h, the accumulation of activity decreased to low levels in all organs but remained higher in the kidneys and in tumor (1.7 ± 0.3 and 1.4 ± 0.3 %ID/g, respectively). Less than 1 %ID/g remained in all organs after 24 h. The biodistribution results are presented in Figure 6. Tumor-to-nontumor ratios for all time points were calculated (Table 2). At 1.5 and 5 h after injection, similar ratios were obtained. The highest ratios were found at 15 h after injection (tumor-to-blood ratio, 45.4). Tumor-to-kidney, tumor-to-liver, and tumor-to-intestine ratios at that time point were 0.8, 2.2, and 5.5, respectively. Although the ratios decreased at 24 h after injection, the tumor-to-blood ratios (31.8) were still somewhat high (Table 2).

In the blockade studies, a dose of 0.3 mg NT-II per mouse significantly decreased uptake of $^{99m}\text{Tc}(\text{CO})_3\text{NT-VIII}$. Uptake was reduced only in tissues rich in the NT receptor (tumor, intestine); accumulation in other organs was not affected, showing the specificity of *in vivo* uptake of $^{99m}\text{Tc}(\text{CO})_3\text{NT-VIII}$ (Fig. 8).

DISCUSSION

NT-VIII, a new NT(8-13) derivative with a change in sequence to prevent enzymatic degradation, was synthesized. This pseudopeptide belongs to a series of NT derivatives, some of which have already been reported (25,27). Here, we described the preclinical evaluation of this new, promising compound. The NT-VIII molecule (Fig. 1) includes (N α His)Ac as a tridentate ligand for labeling with $^{99m}\text{Tc}(\text{CO})_3$ and $^{187}\text{Re}(\text{CO})_3$. (N α His)Ac forms a 5- and 6-membered chelate ring if it is bound to the metal center (technetium or rhenium) with the nitrogen and oxygen atoms, which are shown in boldface in Figure 1. This ring size is much more favorable than a 12- or 14-membered ring, which would be formed if the Arg or the Lys were bound to the metal instead of the aliphatic amine. This is well in accordance with the preserved affinity of the labeled NT-VIII.

The metabolic stability of this new derivative was analyzed *in vitro* both in human plasma and in human colon adenocarcinoma HT-29 cells using a concentration of 0.2 pmol/mL of peptide—the concentration reached in our *in vivo* assays. NT-VIII was highly stable in plasma, and most

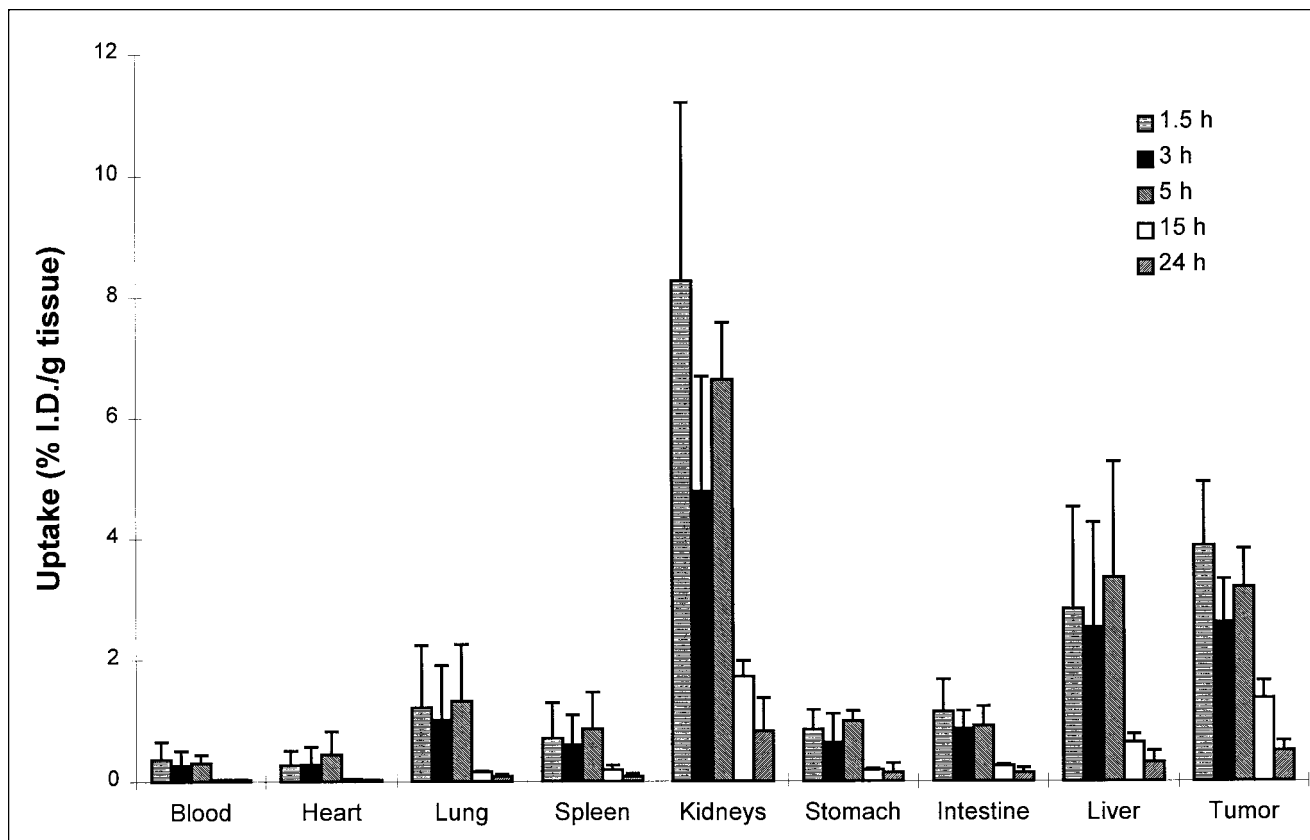


FIGURE 6. Biodistribution in nude mice bearing HT-29 tumor xenografts at different time points after intravenous injection of $^{99m}\text{Tc}(\text{CO})_3\text{NT-VIII}$ (3.5–4 MBq/mouse). Data are %ID/g by reference to total injected dose. Each bar represents mean \pm SD of 3–6 animals.

of the peptide still remained intact after 24 h at 37°C (Fig. 2). This higher stability toward metabolic degradation indicates that stabilization of bond 11–12 is more important than stabilization of bond 8–9. The nonstabilized analog NT-II showed a half-life of 5 min (25), which increased to only 7 min after stabilization of bond 8–9 (analog NT-VI). In contrast, HT-29 cells showed a higher metabolic activity than did human plasma, with more than half of the peptide metabolized at 24 h (Fig. 2). This finding indicates that HT-29 cells contain more specific enzymes for fragment NT(8–13) than does plasma. Receptor-mediated internalization followed by endopeptidase cleavage may be a probable degradation route for this analog in HT-29 cells, as Mentlein and Dahms described for astrocytes (30). Nevertheless, in both systems, the half-life of $^{99m}\text{Tc}(\text{CO})_3\text{NT-VIII}$ was long, showing that all the modifications introduced in fragment NT(8–13) made the molecule highly stable.

The new, stabilized molecule also retained the binding properties. Unlabeled NT-VIII showed lower affinity for NTR1 in HT-29 cells than for NT(8–13), with an approximately 15 times higher IC_{50} (Fig. 3). However, in saturation experiments, similar K_d values were obtained for both $^{99m}\text{Tc}(\text{CO})_3\text{NT-VIII}$ and $^{125}\text{I-NT}$ (1.8 vs. 1.6 nmol/L, Table 1). The affinity of NT-VIII for NTR1 seemed to improve after labeling. This fact was confirmed in inhibition exper-

iments performed with the surrogate $^{\text{nat}}\text{Re}(\text{CO})_3\text{NT-VIII}$, which showed better affinity than did unlabeled NT-VIII (IC_{50} , 7.3 vs. 21.1 nmol/L, Table 1). Similar results were obtained with the less stabilized peptides from the same series (25), which also showed better affinities after labeling, especially in the case of the analog NT-VI (IC_{50} , 23 nmol/L; K_d , 0.5 nmol/L).

As previously described (28,29), NT was rapidly internalized into the cells after binding to the receptors. The internalization was dependent on both time and temperature. At 4°C, no internalization was observed after 2 h of incubation because most of the activity associated with the cells corresponded to surface-bound peptide. Subsequent incubation at 37°C produced a time-dependent increase in internalization reaching a maximum (>90%) after 30 min, at which it remained stable for at least 2 h (Fig. 4). NT-VIII showed internalization properties similar to those of the previously reported NT analogs (25). The percentages of bound peptide as related to the total added were also different at 4°C and 37°C. Thus, after an incubation of 2 h at 4°C, only 0.2% of the total activity added was bound to the cells, whereas after 2 h at 37°C the value increased to 10.3%. This finding shows that, besides the blockade of the internalization, at 4°C the binding of the peptide to the receptor had also decreased. Receptor internalization in-

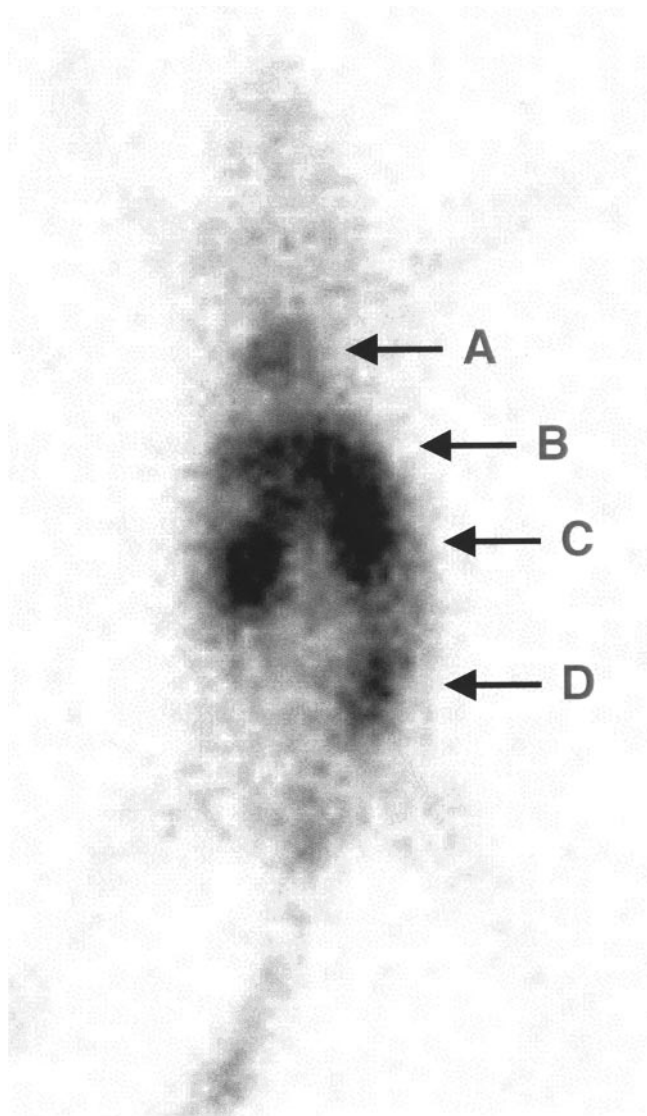


FIGURE 7. Scintigraphy image of mouse bearing tumor xenografts 1.5 h after intravenous injection of $^{99m}\text{Tc}(\text{CO})_3\text{NT-VIII}$ (3.5–4 MBq) shows human colon adenocarcinoma HT-29 xenograft (A), liver (B), kidneys (C), and human prostate carcinoma PC-3 xenograft (D). Tumors were induced by subcutaneous injection of 8×10^6 cells of each type 10 d before assay.

duced by both NT(8–13) and NT-VIII resulted in a decrease in cell-surface NTR1 density. The receptor downregulation in response to high extracellular concentrations of the peptide has been described for NT in HT-29 cells (31) and in rat primary cultured neurons (24). The reduction in the binding capacity on HT-29 cells was lower after incubation with NT-VIII than after incubation with the parent NT(8–13). Reappearance of the receptors on the cell surface was also different (Fig. 5). Maximal recovery was obtained for NT-VIII after 4 h, whereas a longer time was needed for NT(8–13). These differences in downregulation could stem from a lower affinity of unlabeled NT-VIII for NTR1, compared with the affinity for NT(8–13).

Biodistribution was analyzed in nude mice bearing human HT-29 xenografts. $^{99m}\text{Tc}(\text{CO})_3\text{NT-VIII}$ was rapidly distributed and cleared from the blood pool. At 1.5 h after injection, the highest uptake was found in the kidneys (8.3 ± 2.9 %ID/g) and in tumor (3.9 ± 1.1 %ID/g). Accumulation in the other organs tested was not so remarkable (Fig. 6). The high tumor uptake obtained with $^{99m}\text{Tc}(\text{CO})_3\text{NT-VIII}$ allowed clear visualization of tumors by scintigraphy (Fig. 7). At 3 h after injection, uptake was low except in the kidneys, liver, and tumor. After 5 h, accumulation slightly increased, especially in the kidneys, liver, and tumor (Fig. 6). Finally, <1 %ID/g was found in all tissues at 24 h after injection. The best tumor-to-nontumor ratios were obtained at 15 h after injection (Table 2). However, tumor-to-kidney ratios were somewhat low, in this case <1 at all time points tested. The biodistribution in normal tissues did not change significantly compared with what has been reported for other analogs that include the same tridentate ligand in their structure (25). However, tumor uptake was higher, leading to much higher tumor-to-nontumor ratios. The increase in stability allowed more intact peptide to reach the target and bind to the receptors, leading to an increased tumor-to-blood ratio. For instance, for the double-stabilized analog NT-VIII, after 1.5 h the tumor-to-blood ratio was 15, a value that is much higher than those found for the monostabilized analog NT-VI (ratio of 3) and the nonstabilized analog NT-II (ratio of 1) (25).

Blockade experiments were performed to determine whether uptake in tumor was caused by interaction with NTR1. In these experiments, animals received $^{99m}\text{Tc}(\text{CO})_3\text{NT-VIII}$ coinjected with (N α His)Ac-NT(8–13), the analog NT-II from the same series, which also showed a high affinity for NTR1 (25,27). Tumor uptake was significantly reduced from 3.5 %ID/g in the control group (non-blocked) to 0.5 %ID/g in the blocked group (Fig. 8). Also significant was the decreased intestinal accumulation, which was expected because of the evidence that has been found of NTR1 expression in the intestine (32). Uptake in the remaining organs was similar in both groups (nonblocked and

TABLE 2
Tumor-to-Nontumor Ratios in Nude Mice with HT-29 Tumor Xenografts After Intravenous Injection of 3.5–4 MBq $^{99m}\text{Tc}(\text{CO})_3\text{NT-VIII}$

Time after injection (h)	Tu/Bl	Tu/Ki	Tu/Li	Tu/In
1.5	14.8 ± 8.7	0.5 ± 0.2	1.5 ± 0.5	3.3 ± 0.4
3	33.3 ± 4.0	0.7 ± 0.1	1.9 ± 0.1	3.7 ± 0.7
5	15.6 ± 2.0	0.5 ± 0.1	1.8 ± 0.4	4.5 ± 0.9
15	45.4 ± 8.0	0.8 ± 0.2	2.2 ± 0.5	5.5 ± 0.6
24	31.8 ± 14.0	0.8 ± 0.3	2.1 ± 1.0	3.9 ± 0.9

Tu = tumor; Bl = blood; Ki = kidney; Li = liver; In = intestine. Data are mean \pm SD of individual ratios ($n = 3$ –6 animals).

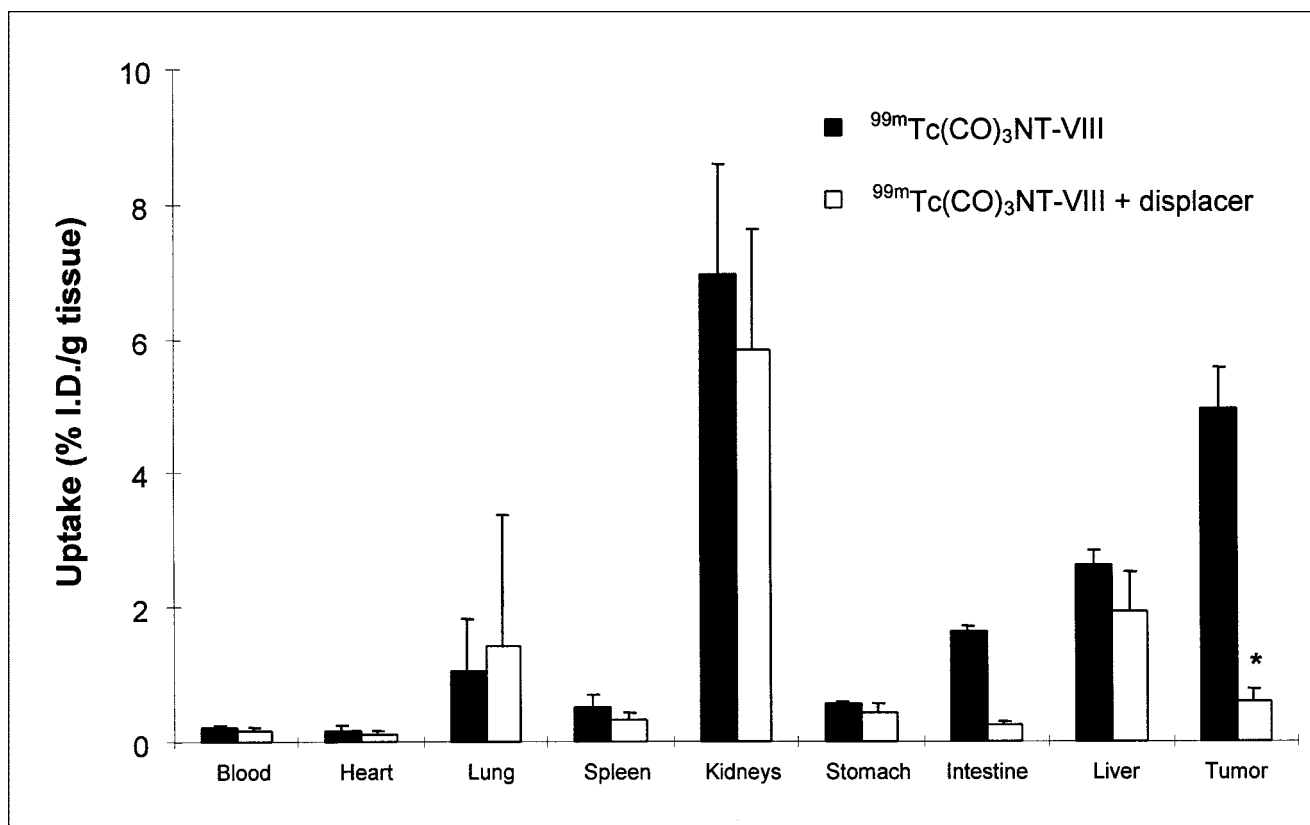


FIGURE 8. Biodistribution of $^{99m}\text{Tc}(\text{CO})_3\text{NT-VIII}$ (3.5–4 MBq/mouse) at 1.5 h after injection after blockade of NTR1. Data are %ID/g by reference to total dose injected and represent mean \pm SD ($n = 3$ –6). Displacer = $(\text{N}\alpha\text{His})\text{Ac-NT}(8$ –13) administered intravenously at dose of 0.3 mg/mouse. * $P < 0.01$, t test.

blocked). We conclude that the increased tumor uptake was caused by specific interaction with NTR1.

Although the densest concentration of NT receptors is in the brain, it showed negligible uptake in our experiments. Heyl et al. (20) reported central activity after systemic administration for this sequence and suggested that it could cross the blood–brain barrier. However, we found no radioactivity in the brain after intravenous administration of $^{99m}\text{Tc}(\text{CO})_3\text{NT-VIII}$, indicating the inability of NT-VIII to cross the blood–brain barrier in mice.

CONCLUSION

With all the results described in this study on the biologic properties of NT-VIII, an NT(8–13) analog, we can conclude that all the modifications introduced in the native NT(8–13) molecule made the new compound more stable without affecting binding properties. Technetium-labeled NT-VIII exhibits a high in vivo tumor uptake that allows scintigraphic tumor imaging of NTR1-bearing neuroendocrine tumors in mice. This promising pseudopeptide may be a good candidate for application in nuclear medicine and has been considered for clinical studies, with the first tests soon to be performed.

ACKNOWLEDGMENTS

The authors thank René Bugmann for technical assistance and Dr. Roger Schibli (Radionuclide Chemistry Group at Paul Scherrer Institute) for supplying the starting material for the Re-NT-VIII synthesis $[\text{NEt}_4]_2[\text{ReBr}_3(\text{CO})_3]$. This study was partly funded by Biomed 2 project BMH4-CT98-3198 and by Fonds voor Werenschappelyk Onderzoek (Fund for Scientific Research) grant G 0.0116.97.

REFERENCES

1. Fischman AJ, Babich JW, Strauss HW. A ticket to ride: peptide radiopharmaceuticals. *J Nucl Med.* 1993;34:2253–2263.
2. Reubi JC. Regulatory peptide receptors as molecular targets for cancer diagnosis and therapy. *Q J Nucl Med.* 1997;41:63–70.
3. McAfee JG, Neumann RD. Radiolabeled peptides and other ligands for receptors overexpressed in tumor cells for imaging neoplasms. *Nucl Med Biol.* 1996;23:673–676.
4. Virgolini I, Raderer M, Kurtaran A, et al. Vasoactive intestinal peptide-receptor imaging for the localization of intestinal adenocarcinomas and endocrine tumours. *N Engl J Med.* 1994;331:1116–1121.
5. Safavy A, Khazaeli MB, Qin H, et al. Synthesis of bombesin analogues for radiolabeling with rhenium-188. *Cancer.* 1997;80:2354–2359.
6. van Hagen PM, Breeman WAP, Reubi JC, et al. Visualization of the thymus by substance P receptor scintigraphy in man. *Eur J Nucl Med.* 1996;23:1508–1513.
7. Behr TM, Jenner N, Radetzky S, et al. Targeting of cholecystokinin-B/gastrin receptors *in vivo*: preclinical and initial clinical evaluation of the diagnostic and therapeutic potential of radiolabelled gastrin. *Eur J Nucl Med.* 1998;25:424–430.
8. Behr TM, Jenner N, Béhé M, et al. Radiolabeled peptides for targeting chole-

- cystokinin-B/gastrin receptor-expressing tumors. *J Nucl Med.* 1999;40:1029–1044.
9. Carraway RE, Leeman SE. The isolation of a new hypotensive peptide, neurotensin from bovine hypothalamus. *J Biol Chem.* 1973;248:6854–6861.
 10. Nemeroff CB, Luttinger D, Prange AJJ. Neurotensin: central nervous system effects of a neuropeptide. *Trends Neurosci.* 1980;3:212–215.
 11. Vincent P. Neurotensin receptors: binding properties, transduction pathways and structure. *Cell Mol Neurobiol.* 1995;15:501–512.
 12. Kitabgi P. Effects of neurotensin on intestinal smooth muscle: application to the study of structure-activity relationships. *Ann N Y Acad Sci.* 1982;400:37–44.
 13. Labbé-Jullié C, Dubuc I, Brouard A, et al. *In vivo* and *in vitro* structure-activity studies with peptide and pseudopeptide neurotensin analogs suggest the existence of distinct central neurotensin receptor subtypes. *J Pharmacol Exp Ther.* 1994; 268:328–336.
 14. Tyler BM, Cusack B, Douglas CL, et al. Evidence for additional neurotensin receptor subtypes: neurotensin analogs that distinguish between neurotensin-mediated hypothermia and antinociception. *Brain Res.* 1998;792:246–252.
 15. Schotte A, Leysen JE, Laduron PM. Evidence for a displaceable non-specific [³H]-neurotensin binding site in rat brain. *Naunyn Schmiedeberg Arch Pharmacol.* 1986;333:400–405.
 16. Vincent JP, Mazella P, Kitabgi P. Neurotensin and neurotensin receptors. *Trends Pharmacol Sci.* 1999;20:302–309.
 17. Reubi JC, Waser B, Schaer JC, Laissue JA. Neurotensin receptors in human neoplasms: high incidence in Ewing's sarcomas. *Int J Cancer.* 1999;82:213–218.
 18. Kitabgi P, De Nadai F, Rovère C, et al. Biosynthesis, maturation, release and degradation of neurotensin and neuromedin N. *Ann N Y Acad Sci.* 1992;668:30–42.
 19. Davis TP, Konings PNM. Peptidases in the CNS: formation of biologically active, receptor-specific peptide fragments. *Crit Rev Neurobiol.* 1993;7:163–174.
 20. Heyl DL, Seffler AM, He JX, Sawyer TK, et al. Structure-activity and conformational studies of a series of modified C-terminal hexapeptide neurotensin analogues. *Int J Peptide Protein Res.* 1994;44:233–238.
 21. Schibli R, La Bella R, Alberto R, et al. Influence of the denticity of ligand systems on the *in vitro* and *in vivo* behavior of ^{99m}Tc(I)-tricarboxyl complexes: a hint for the future functionalization of biomolecules. *Bioconjug Chem.* 2000;11: 345–351.
 22. Alberto R, Egli A, Abram U, et al. Synthesis and reactivity of [NEt₄][ReBr₃(CO)₃]: formation and structural characterization of the clusters [NEt₄][Re₂(μ₃-OH)(μ-OH)₃(CO)₉] and [NEt₄][Re₂(μ-OH)₃(CO)₆] by alkaline titration. *J Chem Soc Dalton Trans.* 1994;2815–2820.
 23. Bauer R, Pabst H-W. Tc-generators: yield of ^{99m}Tc and ratio to inactive ⁹⁹Tc. *Eur J Nucl Med.* 1982;7:35–36.
 24. De Jong M, Berbarud BF, De Bruin E, et al. Internalization of radiolabelled [DTPA⁰]octreotide and [DOTA, Tyr³]octreotide: peptides for somatostatin receptor targeted scintigraphy and radionuclide therapy. *Nucl Med Commun.* 1998;19: 283–288.
 25. García Garayoa E, Allemann-Tannahill L, Bläuenstein P, et al. *In vitro* and *in vivo* evaluation of new radiolabeled neurotensin(8-13) analogues with high affinity for NT1 receptors. *Nucl Med Biol.* 2001;28:75–84.
 26. Hermans E, Vanisberg MA, Geurts M, et al. Down-regulation of neurotensin receptors after ligand-induced internalization in rat primary culture neurons. *Neurochem Int.* 1997;31:291–299.
 27. Schubiger PA, Allemann-Tannahill L, Egli A, et al. Catabolism of neurotensins: implications for the design of radiolabeling strategies of peptides. *Q J Nucl Med.* 1999;43:155–158.
 28. Hermans E, Octave JN, Maloteaux JM. Receptor mediated internalization of neurotensin in transfected Chinese hamster ovary cells. *Biochem Pharmacol.* 1994;47:89–91.
 29. Mazella JE, Leonard K, Chabry J, et al. Binding and internalization of iodinated neurotensin in neuronal cultures from embryonic mouse brain. *Brain Res.* 1991; 564:249–255.
 30. Mentlein R, Dahms P. Endopeptidases 24.16 and 24.15 are responsible for the degradation of somatostatin, neurotensin and other neuropeptides by cultivated rat cortical astrocytes. *J Neurochem.* 1994;62:27–36.
 31. Turner JT, James-Kracke MR, Camden JM. Regulation of the neurotensin receptor and intracellular calcium mobilization in HT-29 cells. *J Pharmacol Exp Ther.* 1990;253:1049–1056.
 32. Tanaka K, Masu M, Nakanishi S. Structure and functional expression of the cloned rat neurotensin receptor. *Neuron.* 1990;4:847–854.

